

Effects of post-annealing and cobalt co-doping on superconducting properties of (Ca,Pr)Fe₂As₂ single crystals

T. Okada, H. Ogino, H. Yakita, A. Yamamoto, K. Kishio, J. Shimoyama

Department of Applied Chemistry, University of Tokyo, 7-3-1 Hongo, Bunkyo-ku, Tokyo 113-8656, Japan

ABSTRACT

In order to clarify the origin of anomalous superconductivity in (Ca,RE)Fe₂As₂ system, Pr doped and Pr,Co co-doped CaFe₂As₂ single crystals were grown by the FeAs flux method. These samples showed two-step superconducting transition with $T_{c1} = 25\sim 42$ K, and $T_{c2} < 16$ K, suggesting that (Ca,RE)Fe₂As₂ system has two superconducting components. Post-annealing performed for these crystals in evacuated quartz ampoules at various temperatures revealed that post-annealing at $\sim 400^\circ\text{C}$ increased the *c*-axis length for all samples. This indicates that as-grown crystals have a certain level of strain, which is released by post-annealing at $\sim 400^\circ\text{C}$. Superconducting properties also changed dramatically by post-annealing. After annealing at 400°C , some of the co-doped samples showed large superconducting volume fraction corresponding to the perfect diamagnetism below T_{c2} and high J_c values of $10^4\sim 10^5$ Acm⁻² at 2 K in low field, indicating the bulk superconductivity of (Ca,RE)Fe₂As₂ phase occurred below T_{c2} . On the contrary, the superconducting volume fraction above T_{c2} was always very small, suggesting that 40 K-class superconductivity observed in this system is originating in the local superconductivity in the crystal.

1. Introduction

Various iron-based superconductors consisting of superconducting FePn(Ch) and blocking layers have been discovered since 2008[1-7]. Among these compounds, ‘122’ family (AEFe₂As₂ ; AE = alkaline earth metals) attracts intense attention even from a practical viewpoint because of its relatively high T_c and low anisotropy. RE doped CaFe₂As₂ (RE = La, Ce, Pr and Nd)[8] shows highest T_c in the 122 family, up to 49 K for RE = Pr[9]. In addition, La,P co-doped CaFe₂As₂ single crystal was reported to show high T_c (~ 45 K) and a large superconducting volume fraction at 5 K[10].

However, the origin of the superconductivity in (Ca,RE)Fe₂As₂ is still controversial due to its anomalous superconducting properties, such as its small superconducting volume fraction above 20 K[8,9,11], larger anisotropy compared with other 122 compounds[12], and two-step

superconducting transition[9,12-15]. Furthermore, any superconducting behavior has not been observed in thin films or polycrystalline samples of $(Ca,RE)Fe_2As_2$. No superconducting single-crystalline $(Ca,RE)Fe_2As_2$ grown by the Sn flux method is reported, either, although weak superconductivity with T_c exceeding 40 K is reproducibly observed in single crystals grown by the FeAs flux method[8,9,11]. Therefore, the origin of the superconductivity in $(Ca,RE)Fe_2As_2$ remains unclear and contributions of interface effect accompanied by local strain originating in As vacancy[16,17] or inhomogeneous distribution of dopants[14] are recently proposed.

In order to clarify the origin of superconductivity in $(Ca,RE)Fe_2As_2$, Pr doped and Pr,Co co-doped $CaFe_2As_2$ single crystals were grown by FeAs flux method. Their superconducting properties including the post-annealing effect were studied, because structural, magnetic and superconducting properties of undoped and Co-doped $CaFe_2As_2$ single crystals grown by the FeAs flux method can be controlled by post-annealing[18-20]. Structural and superconducting properties of Pr doped and Pr,Co co-doped $CaFe_2As_2$ samples were evaluated through X-ray diffraction and magnetic susceptibility measurements.

2. Experimental

Single crystals of $CaFe_2As_2$ were grown by the FeAs self-flux method with nominal compositions of $(Ca_{1-x}Pr_x)(Fe_{1-y}Co_y)_4As_4$. According to the nominal Pr and Co compositions x and y , samples were labeled as sample 1 ~ sample 8, which are listed in Table 1. In a glove box filled with high purity Ar gas, Ca shots (Alfa Aesar, 99%) were shaved using a file and mixed with FeAs (Furukawa Electric 99.9%), CoAs (Furukawa Electric 99.9%), and Pr (Kojundo Chemical Laboratory, 99.9%) powders. The mixture was pelletized, loaded into an alumina tube and sealed in an evacuated quartz ampoule. The quartz ampoule was heated to 1000°C in 4 hours, kept at 1000°C for 36 hours and slowly cooled down to 950°C in 50 hours, then it was cooled down to room temperature by switching off the furnace. Plate-like single crystals of $CaFe_2As_2$ were mechanically separated from the flux. Some of the as-grown crystals were sealed in evacuated quartz ampoules again and annealed at various temperatures ranging from 300 to 600°C for 3~7 days followed by quenching to room temperature. The constituent phases of the samples were analyzed by X-ray diffraction measurement (RIGAKU Ultima-IV) with $Cu-K_\alpha$ radiation generated at 40 kV and 40 mA. Silicon powder was used as an internal standard to determine the c -axis length of the $CaFe_2As_2$ crystal. Magnetization measurements were performed by a SQUID magnetometer (Quantum Design MPMS-XL5s). J_c was calculated from the width of magnetization hysteresis based on the extended Bean model, $J_c [A\ cm^{-2}] = 20 \Delta M(H) / (a - a^2/3b)$, where $\Delta M(H) [emu\ cm^{-3}] = M^+(H) - M(H)$ ($M(H)$ and $M^+(H)$ are magnetizations measured with field increasing and decreasing, respectively) and a [cm] and b

[cm] are lengths of shorter and longer edges of the rectangular crystal.

3. Results and discussion

Plate-like single crystals of $(\text{Ca}_{1-x}\text{Pr}_x)(\text{Fe}_{1-y}\text{Co}_y)_2\text{As}_2$ with flat shiny surface were successfully grown. Their typical dimensions were $\sim 3 \times 3 \times 0.2$ ($//c$) mm^3 . Fig. 1(a) shows surface XRD patterns, where only sharp $00l$ peaks are observed. A single diffraction of peak for each hkl index without splitting (See Fig. 1(b) for sample 8) indicates absence of phase separation with different dopant concentrations. In addition, systematic decrease in c -axis length with increasing nominal x and y as shown in Fig. 2(a) suggests that doping levels of both Pr and Co are successfully controlled.

For annealed crystals, the value of full width at half maximum (FWHM) of 008 peak seemed to be smaller. In addition, c -axes of the samples annealed at 400°C are longer than those of as-grown ones as shown in Fig. 2(a), while samples annealed at $\sim 600^\circ\text{C}$ have comparable or shorter c -axes compared with as-grown ones as indicated in Fig. 1(b) and 2(b). This peculiar increase in c -axis length after annealing at 400°C has also been reported in undoped[18,20] and Co-doped[19] CaFe_2As_2 single crystals grown by the FeAs flux method. In these previous reports, as-grown CaFe_2As_2 single crystals grown out of FeAs flux are considered to have some strains, which decrease the lattice volume as external pressure does. Our results indicate that as-grown Pr-doped and Pr,Co co-doped CaFe_2As_2 crystals grown by the FeAs flux method also have the strain. This strain is released by annealing at $\sim 400^\circ\text{C}$, and it reappears by annealing at $\sim 600^\circ\text{C}$.

Fig. 3(a) shows ZFC magnetization curves for a Pr-doped CaFe_2As_2 crystal, sample 2, where magnetic field is applied parallel to the c -axis. The as-grown sample showed superconductivity with T_c of ~ 42 K. However, the superconducting transition was very broad and the diamagnetic signal is not large enough to ensure the bulk superconductivity considering its large demagnetization factor corresponding to the plate-like shape of the crystal. When magnetic field is applied parallel to the c -axis of the crystal with dimensions of $\sim 3 \times 3 \times 0.2$ ($//c$) mm^3 , the demagnetization factor is roughly estimated to be ~ 0.90 , by approximating the crystal shape by an ellipse, and diamagnetism of $4\pi M/H \sim -10$ corresponds to full shielding in this case.

After annealing at 400°C superconductivity in sample 2 almost disappeared, while very weak diamagnetism was observed below 8 K. Interestingly, superconductivity of the crystal recovered by annealing at 600°C . This can be attributed to the release and regeneration of strains in the crystal by post-annealing at 400°C and 600°C , respectively. On the other hand, the superconducting volume fraction of a Pr,Co co-doped CaFe_2As_2 crystal, sample 8, became larger after annealing at 400°C as shown in Fig. 3(b). For sample 2 and 8, four samples each were measured to confirm reproducibility of the annealing effect, and they showed very similar

behaviors. Other Pr,Co co-doped crystals (sample 3~7) also maintained superconductivity even after annealing at 400°C. In these Pr,Co co-doped crystals, T_c s were almost unchanged before and after annealing. The superconducting property of BaFe₂As₂ under external pressure gives us a clue to understand this behavior. In the cases of BaFe₂As₂ crystals doped with K, P or Co, underdoped samples show large enhancement of T_c under external pressure, while optimally-doped or overdoped samples does not show such changes of T_c [21-23]. Hence, we consider that sample 2 was in the underdoped state and therefore it showed large change in superconducting properties before and after annealing at 400°C. On the contrary, in Pr,Co co-doped samples, the electron doping level was intrinsically enhanced by Co substitution for the Fe site, thus superconductivity did not disappear after 400°C annealing.

Fig. 4(a) and (b) show zero-field-cooled (ZFC) magnetization curves of sample 3 and 4, respectively, before and after annealing at 400°C. These measurements were performed under 1 Oe applied parallel to the c -axis. After the annealing, these samples showed two-step superconducting transition at T_{c1} of ~25 K for sample 3 and ~32 K for sample 4 and T_{c2} of 12 K for both samples. These T_{c1} and T_{c2} were determined by the onset of diamagnetic transition and the kink of the field-cooled (FC) magnetization curve, respectively, as indicated by arrows in the inset of Fig. 4. Temperature dependences of ZFC magnetization of these samples were very small up to ~6 K, and the transitions at T_{c2} were sharp. It should be emphasized that the magnitudes of observed ZFC magnetization below 6 K were close to the expected values for full shielding when we take the shapes of the measured samples into account. For sample 3 with $\sim 2.6 \times 1.7 \times 0.1$ (// c) mm³ in dimension, the demagnetization factor is roughly estimated to be ~ 0.93 , and $4\pi M / H \sim -14$ is obtained by assuming the full shielding state. Sample 4 was thicker than the other samples, with dimensions of $\sim 2 \times 2 \times 0.6$ mm³. In this case, the demagnetization factor is estimated to be ~ 0.66 and expected magnetic susceptibility due to perfect diamagnetism is $4\pi M / H \sim -2.9$. These results strongly suggest the bulk superconductivity of annealed sample 3 and 4 below T_{c2} .

The ZFC magnetization curve of the 400°C annealed sample 4 under 1 Oe applied parallel to the ab -plane is shown in Fig. 4(c). Superconducting volume fraction at low temperatures is estimated to be approximately 100 %, which also ensures the bulk superconductivity below T_{c2} . However, as shown in the enlarged view, diamagnetism derived from the high- T_c component is not observed in this set up. This is probably due to granular and anisotropic distribution of high- T_c component, as suggested by F. Y. Wei *et al.* [16], and larger penetration depth than thickness of high- T_c regions.

Fig. 5 shows magnetization hysteresis loops at 2 K of as-grown sample 2 and 400°C annealed sample 3, 4 and 8. Widths of magnetization hysteresis ΔM of sample 2 and 8 were quite small and J_c (2 K, ~ 0 T) of these samples were estimated to be as low as $\sim 1 \times 10^2$ A cm⁻².

This is attributed to weak superconductivity under magnetic field as indicated in the magneto-optical image of $(\text{Ca,Lu})\text{Fe}_2\text{As}_2$ [24]. On the contrary, sample 3 and 4 showed large magnetization hysteresis and their J_c values at 2 K in ~ 0 T were calculated to be $\sim 10^5$ A cm⁻² and $\sim 10^4$ A cm⁻², respectively, which were much higher than that of $(\text{Ca,Lu})\text{Fe}_2\text{As}_2$ [24] and comparable to that of $\text{Ca}(\text{Fe,Co})_2\text{As}_2$ [25]. For sample 4, magnetization hysteresis loops were measured for another sample in order to confirm reproducibility of the bulk superconductivity, and it also showed high J_c , which is shown in Fig. 6, indicating bulk superconductivity below T_{c2} . Therefore, we conclude that sample 3 and 4 annealed at 400°C are bulk superconductors below T_{c2} .

Here we would like to discuss the two-step superconducting transition observed in the samples. For Pr-doped and Co-free samples, two-step transition at $T_{c1} = 42$ K and $T_{c2} = 16$ K was observed in sample 2, while sample 1 did not show clear diamagnetism both before and after annealing possibly due to insufficient carrier concentration. In Pr,Co co-doped samples, sample 3~8 exhibited two-step transition as in the case of sample 4, with $T_{c1} = 25 \sim 36$ K and $T_{c2} < 16$ K. This two-step transition has also been found in La-[12,13] and Pr-doped[9,14,15] samples by both susceptibility and resistivity measurements. Considering these facts, we believe that two-superconducting components coexist in the $(\text{Ca,RE})\text{Fe}_2\text{As}_2$ system.

Our result on sample 3 and 4 indicates that the low- T_c component of this system originates in bulk superconductivity of $(\text{Ca,RE})\text{Fe}_2\text{As}_2$. Fig. 6 shows magnetic field dependences of J_c at 2 K for sample 3~6 annealed at 400°C. For sample 4, we have examined for two crystals as described before. Sample 3 showed very high J_c up to $\sim 10^5$ Acm⁻², while its T_{c1} was relatively low ~ 25 K. On the other hand, the estimated J_c values (at 2 K in low field) for sample 5~8 were $\sim 10^2$ A cm⁻², which is too small to ensure bulk superconductivity. This fact implies that the bulk superconductivity of low- T_c phase can be observed in a very narrow range of electron doping level, which is determined by the nominal composition as well as the heat treatment condition. In the heavily doped samples compared to sample 4 ($x = 0.07$, $y = 0.02$), the superconducting volume fractions at low temperatures are not very small (30 ~ 90 % at 2 K. See Fig. 3(b) for sample 8), whereas their J_c values are quite low. This is probably due to the collapsed tetragonal (CT) phase appeared in the heavily doped compounds and this phase is considered to suppress superconductivity as suggested in Rh-doped CaFe_2As_2 [26]. It should be noted again that any as-grown sample did not show clear bulk superconductivity possibly due to the strain which also degrades superconductivity.

On the other hand, all the samples exhibited very small superconducting volume fraction above T_{c2} even after post-annealing, suggesting that the transition at T_{c1} is due to a local superconductivity in the crystal[12,14,16,17]. It is possible that intergrowth of iron-pnictide superconductor, such as $(\text{Ca,RE})\text{FeAs}_2$ [27,28], is the origin of 40 K-class superconductivity in

this system. However, reported T_c on Pr-doped CaFeAs_2 is as low as 20 K so far[エラー! ブックマークが定義されていません。], while $(\text{Ca},\text{La})\text{FeAs}_2$ [エラー! ブックマークが定義されていません。] and $(\text{Ca},\text{La})\text{Fe}(\text{As},\text{Pn})_2$ ($\text{Pn} = \text{P}, \text{Sb}$)[29] exhibits 40 K-class superconductivity. Further explorations are needed to reveal the origin of the high- T_c component in Ca-RE-Fe-As system.

4. Summary

Pr doped and Pr,Co co-doped CaFe_2As_2 single crystals were successfully grown by FeAs flux method and post-annealing effects on these samples were investigated. Expansion of c -axis after annealing at 400°C indicated existence of strain in the as-grown crystals, which might affect superconducting properties in analogy with external pressure. Superconductivity of Pr doped samples disappeared after 400°C annealing, while Pr,Co co-doped samples maintained superconductivity even after 400°C annealing, suggesting that electron doping level was enhanced by Co substitution for the Fe site. It was revealed that $(\text{Ca},\text{RE})\text{Fe}_2\text{As}_2$ system has two superconducting components through magnetic susceptibility measurements. Large diamagnetisms indicating the full shielding state were observed below T_{c2} in some of the co-doped samples after the annealing and they exhibited high J_c of $10^4\sim 10^5$ A cm^{-2} at 2 K in low field. This results indicate that the low- T_c component ($T_c < 20$ K) is due to bulk superconductivity of $(\text{Ca},\text{RE})\text{Fe}_2\text{As}_2$, while bulk superconductivity was confirmed to appear in a limited electron doping level. On the other hand, any evidences of bulk superconductivity have not been found for high- T_c one thus far, supporting the idea of local superconductivity in the bulky crystal.

Acknowledgement

This work was partially supported by SICORP of Japan Science and Technology Agency (JST).

References

- [1] Y. Kamihara, T. Watanabe, M. Hirano, H. Hosono, J. Am. Chem. Soc. 130 (2008) 329.
- [2] F.C. Hsu, J.Y. Luo, K.W. Yeh, T.K. Chen, T.W. Huang, P.M. Wu, Y.C. Lee, Y.L. Huang, Y.Y. Chu, D.C. Yan, M.K. Wu, Proc. Natl Acad. Sci. 105 (2008) 14262
- [3] X.C. Wang, Q.Q. Liu, Y.X. Lv, W.B. Gao, L.X. Yang, R.C. Yu, F.Y. Li, C.Q. Jin, Solid State Commun. 148 (2008) 538
- [4] M. Rotter, M. Tegel, D. Johrendt, Phys. Rev. Lett. 101 (2008) 107006
- [5] Jaroszynski, S. C. Riggs, F. Hunte, A. Gurevich, D. C. Larbalestier, G. S. Boebinger, F. F. Balakirev, A. Migliori, Z. A. Ren, W. Lu, J. Yang, X. L. Shen, X. L. Dong, Z. X. Zhao, R.

- Jin, A. S. Sefat, M. A. McGuire, B. C. Sales, D. K. Christen, D. Mandrus, *Phys. Rev. B* 78 (2008) 064511.
- [6] H. Ogino, Y. Matsumura, Y. Katsura, K. Ushiyama, S. Horii, K. Kishio, J. Shimoyama, *Supercond. Sci. Technol.* 22 (2009) 075008
- [7] M. Nohara, S. Kakiya, K. Kudo, Y. Oshiro, S. Araki, T.C. Kobayashi, K. Oku, E. Nishibori, H. Sawa, *Solid State Commun.* 152 (2012) 635
- [8] S. R. Saha, N. P. Butch, T. Drye, J. Magill, S. Ziemak, K. Kirshenbaum, P. Y. Zavalij, J. W. Lynn, J. Paglione, *Phys. Rev. B* 85 (2012) 024525.
- [9] B. Lv, L. Deng, M. Gooch, F. Wei, Y. Sun, J. K. Meen, Y. Y. Xue, B. Lorenz, C. W. Chu, *Proc. Natl. Acad. Sci. USA* 108 (2011) 15705
- [10] K. Kudo, K. Iba, M. Takasuga, Y. Kitahama, J. Matsumura, M. Danura, Y. Nogami and M. Nohara, *scientific reports* 3 (2013) 1478
- [11] W. Zhou, Y. Qi, L. Wang, D. Wang, X. Zhang, C. Yao, C. Wang, Y. Ma, *Euro. Phys. Lett.*, 95, 670002 (2011)
- [12] W. Zhou, F. F. Yuan, J. C. Zhuang, Y. Sun, Y. Ding, L. J. Cui, J. Bai, Z. X. Shi, *Supercond. Sci. Technol.* 26 (2013) 095003
- [13] Y. Sun, W. Zhou, L. J. Cui, J. C. Zhuang, Y. Ding, F. F. Yuan, J. Bai, Z. X. Shi, *AIP Advances* 3 (2013) 102120
- [14] K. Gofryk, M. Pan, C. Cantoni, B. Sagarov, J. E. Mitchell, A. S. Sefat, *Phys. Rev. Lett.* 112, 047005 (2014)
- [15] D. Cargill, W. Uhoya, G. Krzysztow, G. M. Tsoi, Y. K. Vohra, A. S. Sefat, S. T. Weir, *arXiv*. 1310. 3842
- [16] F. Y. Wei, B. Lv, L. Z. Deng, J. K. Meen, Y. Y. Xue, J. E. Hoffman and C. W. Chu, *arXiv*. 1309. 0034
- [17] B. Lv, F. Y. Wei, L. Z. Deng, Y. Y. Xue and C. W. Chu, *arXiv*. 1308. 3129
- [18] S. Ran, S. L. Bud'ko, D. K. Pratt, A. Kreyssig, M. G. Kim, W. E. Straszheim, J. Soh, M. J. Kramer, D. H. Ryan, W. N. Rowan-Weetaluktuk, Y. Furukawa, A. I. Goldman, P. C. Canfield, *Phys. Rev. B* 83 (2011) 144517
- [19] S. Ran, S. L. Bud'ko, W. E. Straszheim, J. Soh, M. G. Kim, A. Kreyssig, A. I. Goldman, P. C. Canfield, *Phys. Rev. B* 85 (2012) 224528
- [20] B. Sagarov, C. Cantoni, M. Pan, T. C. Hogan, W. Ratcliff II, S. D. Wilson, K. Fritsch, B. D. Gaulin, A. S. Sefat, *scientific reports* 4 (2014) 4120
- [21] T. Yamazaki, N. Takeshita, K. Kondo, R. Kobayashi, Y. Yamada, H. Fukazawa, Y. Kohori, P. M. Shirage, K. Kihou, H. Kito, H. Eisaki, and A. Iyo, *J. Phys.: Conf. Ser.* **215**, (2010) 012041
- [22] L. E. Klintberg, S. K. Goh, S. Kasahara, Y. Nakai, K. Ishida, M. Sutherland, T. Shibauchi, Y. Matsuda, and T. Terashima, *J. Phys. Soc. Jpn.* **79**, (2010) 123706

- [23] E. Colombier, M. S. Torikachvili, N. Ni, A. Thaler, S. L. Bud'ko, and P. C. Canfield, *Supercond. Sci. Technol.* **23**, (2010) 054003
- [24] T. Tamegai, Q. P. Ding, T. Ishibashi, Y. Nakajima, *Physica C* 484 (2013) 31-34
- [25] A.K. Pramanik, L. Harnagea, S. Singh, S. Aswartham, G. Behr, S. Wurmehl, C. Hess, R. Klingeler, B. Büchner, *Phys. Rev. B* 82 (2010) 014503
- [26] M. Danura, K. Kudo, Y. Oshiro, S. Araki, T. C. Kobayasi, M. Nohara, *J. Phys. Soc. Japan*, 80 (2011) 103701
- [27] H. Yakita, H. Ogino, T. Okada, A. Yamamoto, K. Kishio, T. Tohei, Y. Ikuhara, Y. Gotoh, H. Fujihisa, K. Kataoka, H. Eisaki, J. Shimoyama, *J. Am. Chem. Soc.* 136 (2014) 846-849
- [28] N. Katayama, K. Kudo, S. Onari, T. Mizukami, K. Sugawara, Y. Sugiyama, Y. Kitahama, K. Iba, K. Fujimura, N. Nishimoto, M. Nohara, H. Sawa, *J. Phys. Soc. Jpn.* 82 (2013) 123702
- [29] K. Kudo, T. Mizukami, Y. Kitahama, D. Mitsuoka, K. Iba, K. Fujimura, N. Nishimoto, Y. Hiraoka, M. Nohara, *J. Phys. Soc. Jpn.* 83 (2014) 025001

Figure Captions

Fig. 1 (a) Surface XRD patterns of as-grown sample 2 and 8. The inset shows the photograph of grown single crystal. (b) Enlarged view of the XRD patterns around 64° for as-grown and annealed samples.

Fig. 2 (a) c -axis lengths of as-grown and 400°C -annealed $(\text{Ca}_{1-x}\text{Pr}_x)(\text{Fe}_{1-y}\text{Co}_y)_2\text{As}_2$ single crystals. (b) Effect of annealing temperature on c -axis lengths of sample 2 ($x = 0.14, y = 0$) and 8 ($x = 0.14, y = 0.05$).

Fig. 3 Effect of post-annealing on the superconducting properties of (a) sample 2 ($x = 0.14, y = 0$) and (b) sample 8 ($x = 0.14, y = 0.05$).

Fig. 4 ZFC magnetization curves for sample 3 ($x = 0.05, y = 0.02$) (a) and sample 4 ($x = 0.07, y = 0.02$) (b) before and after annealing at 400°C under $H // c$ and a ZFC magnetization curve of sample 4 measured under $H // ab$ (c). The insets show the enlarged views of the magnetization curves.

Fig. 5 Magnetic hysteresis loops measured at 2 K under $H // c$ for as-grown sample 2 ($x = 0.14, y = 0$) and 400°C annealed crystals of sample 3 ($x = 0.05, y = 0.02$), sample 4 ($x = 0.07, y = 0.02$) and sample 8 ($x = 0.14, y = 0.05$).

Fig. 6 Magnetic field dependences of J_c at 2 K under $H // c$ for sample 3~6 after annealing at 400°C . For sample 4, two crystals indicated as 4a and 4b were measured.

Table 1 Sample labels for $(\text{Ca}_{1-x}\text{Pr}_x)(\text{Fe}_{1-y}\text{Co}_y)_2\text{As}_2$ single crystals

sample #	x	y
1	0.07	0
2	0.14	0
3	0.05	0.02
4	0.07	0.02
5	0.10	0.02
6	0.14	0.02
7	0.07	0.05
8	0.14	0.05

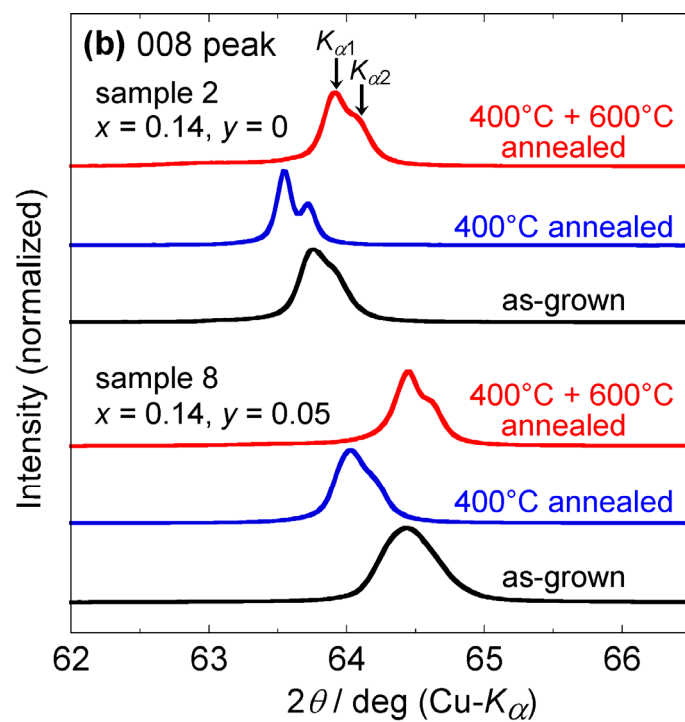
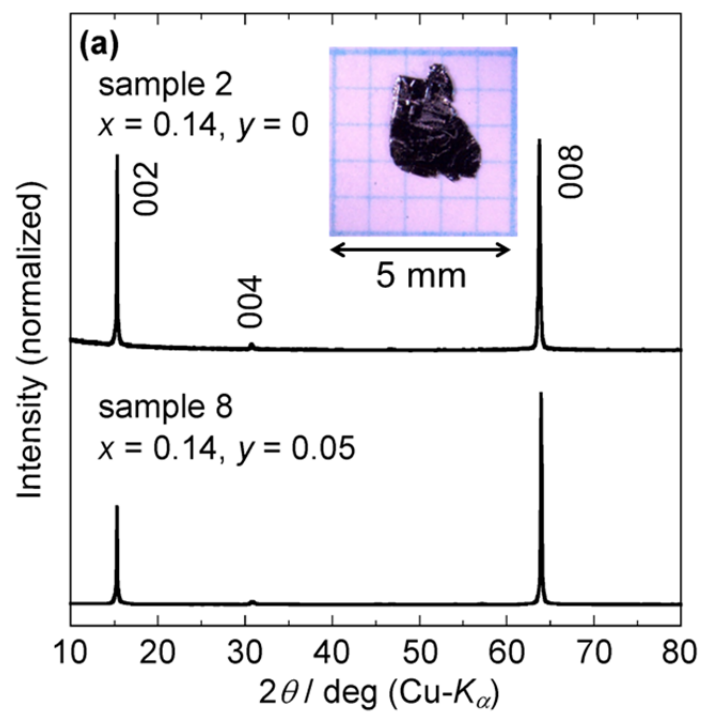


Fig. 1

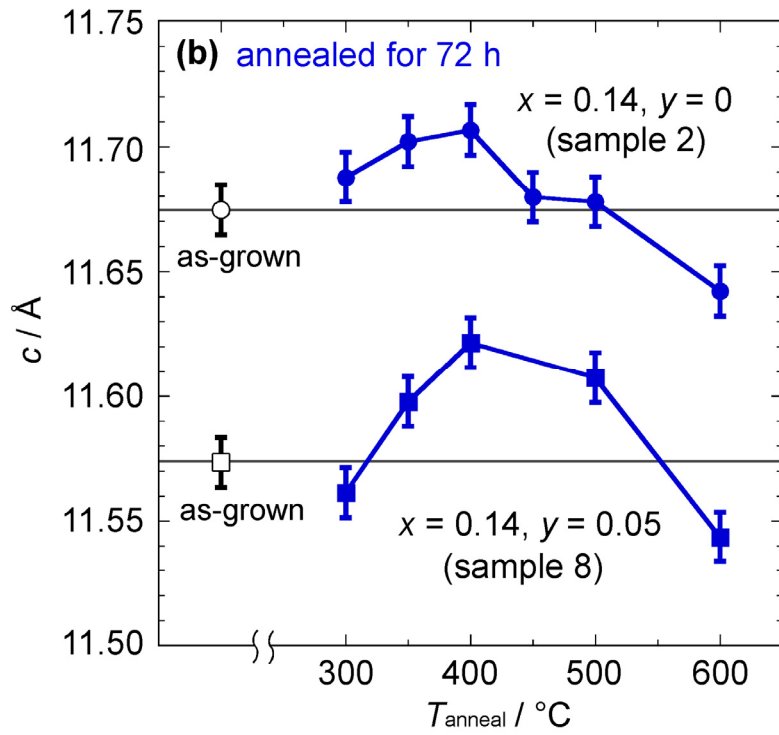
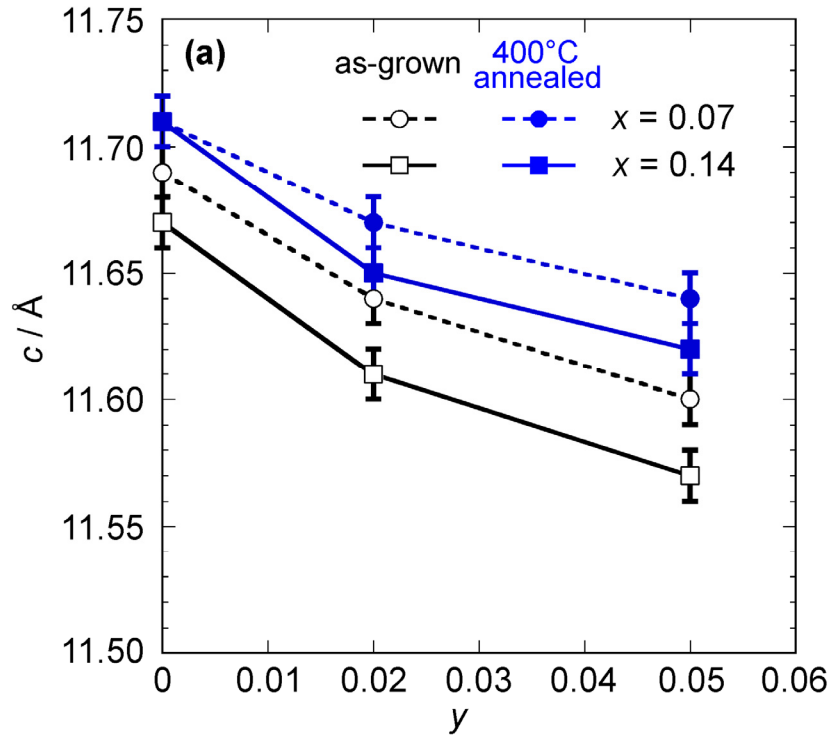


Fig. 2

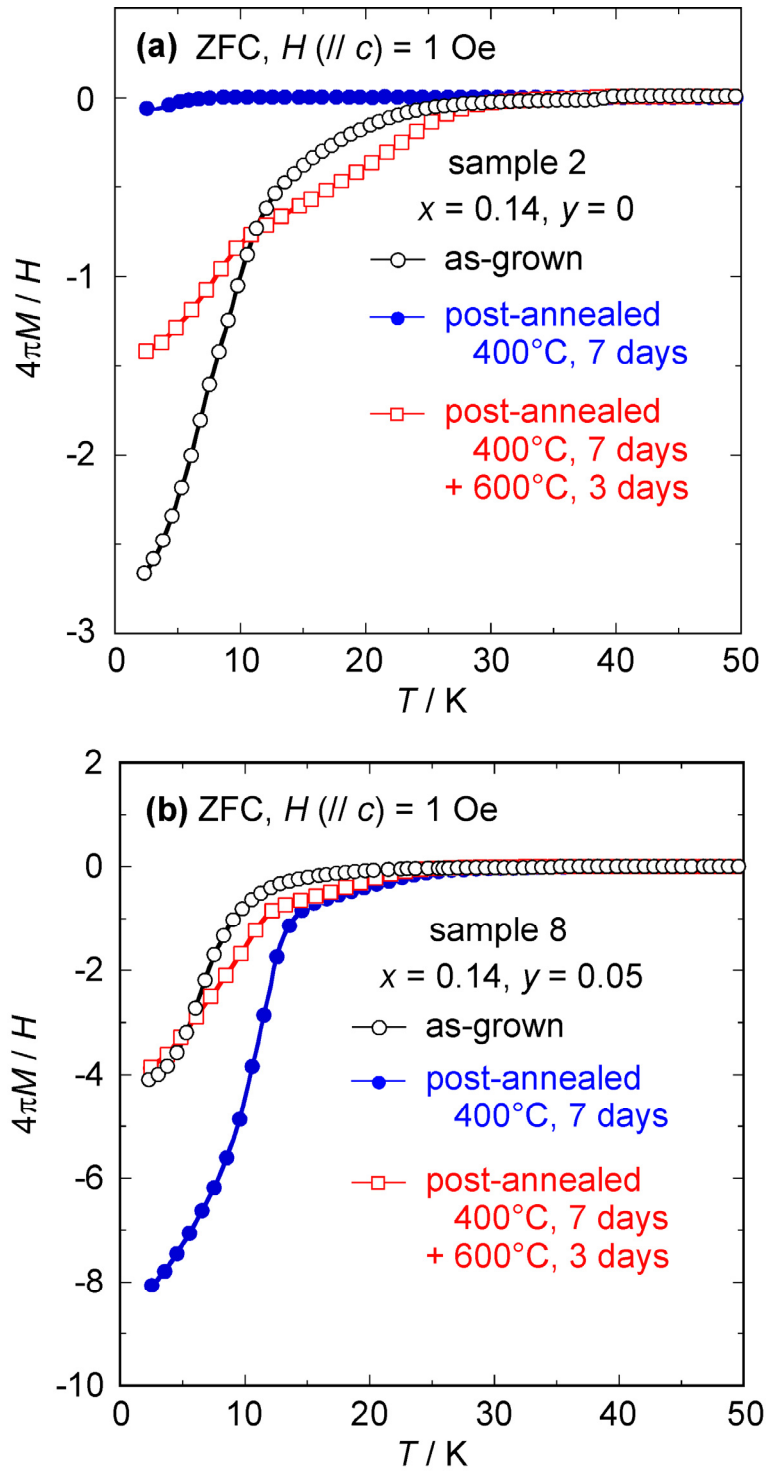
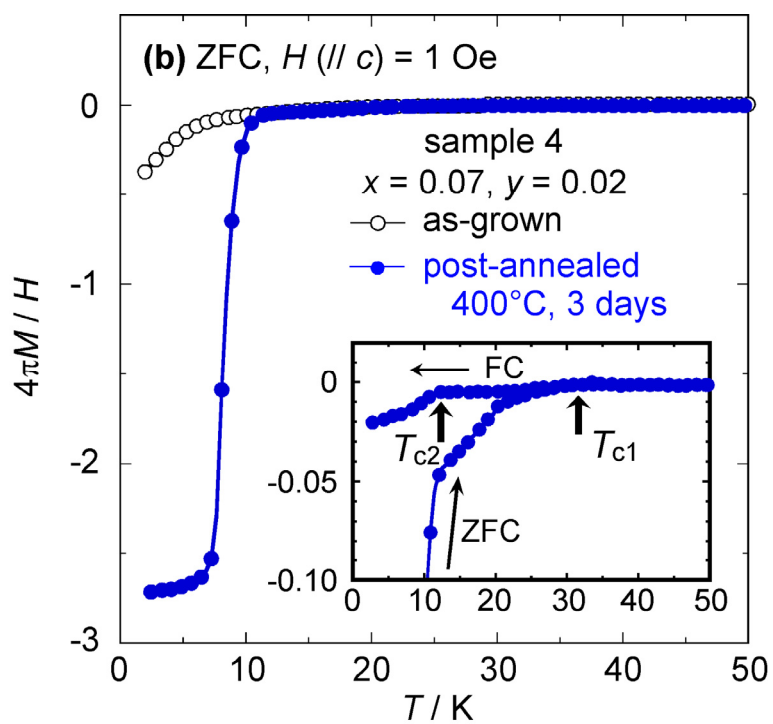
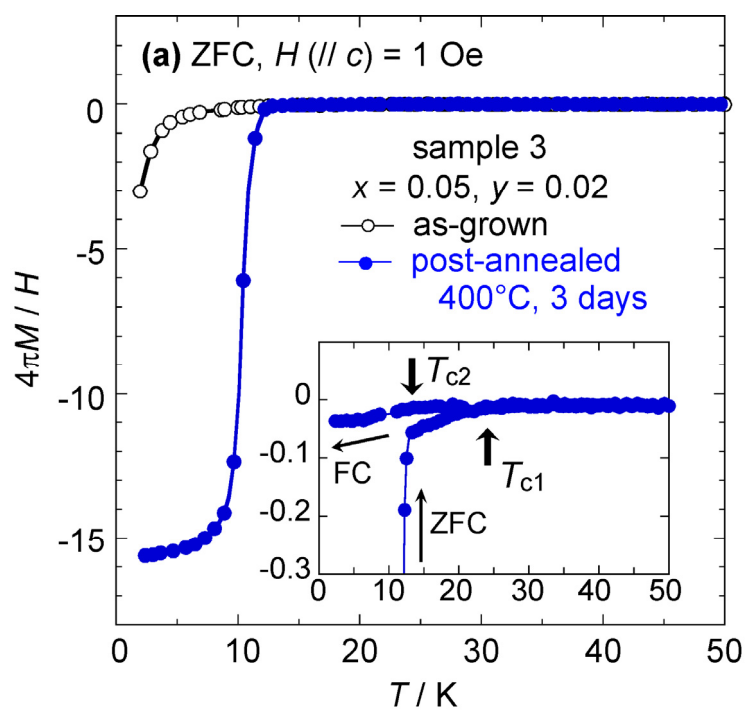


Fig. 3



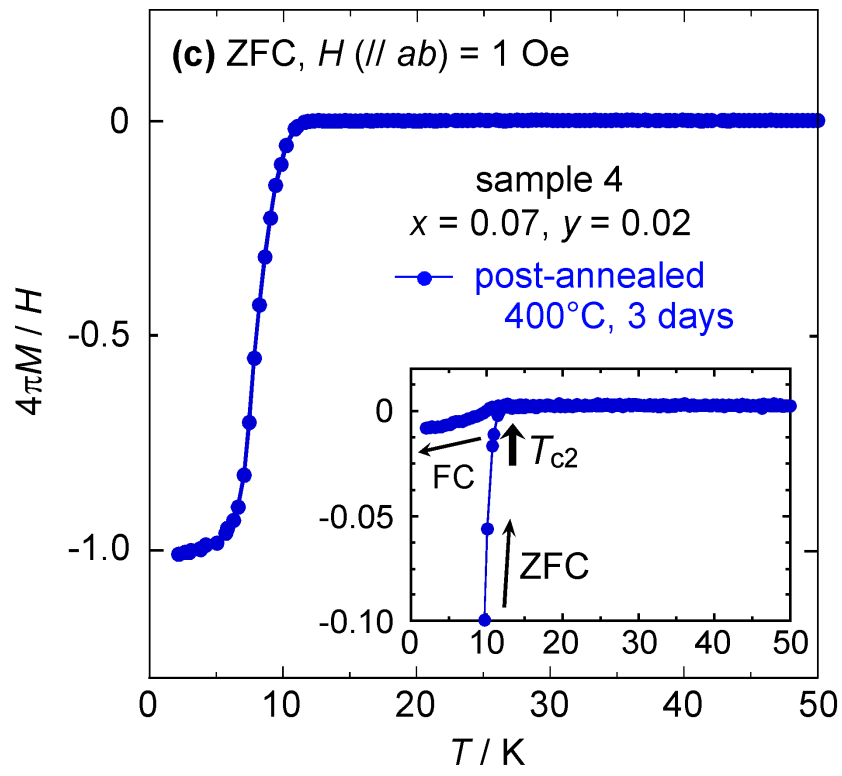


Fig. 4

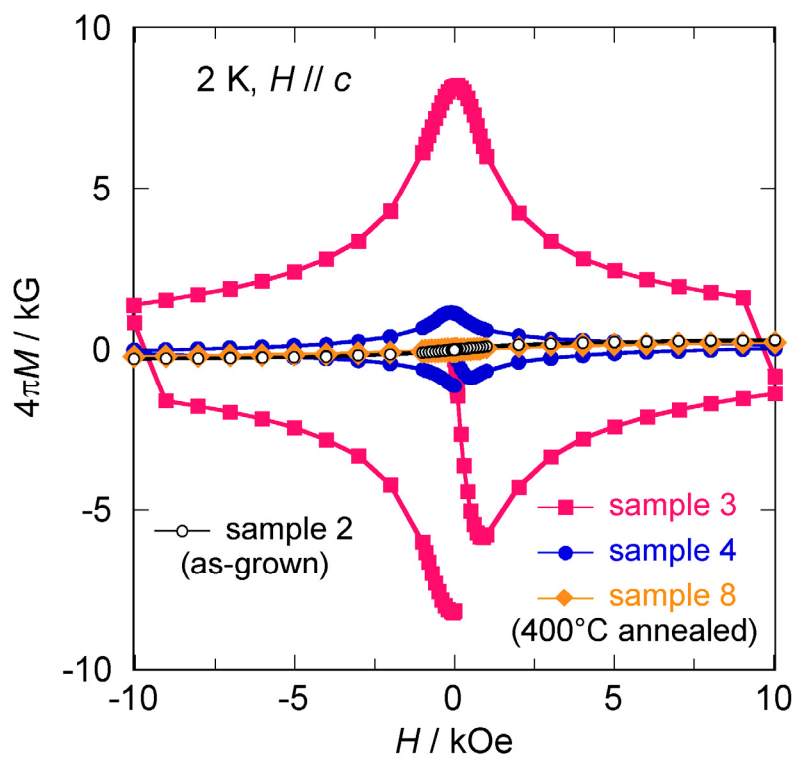


Fig. 5

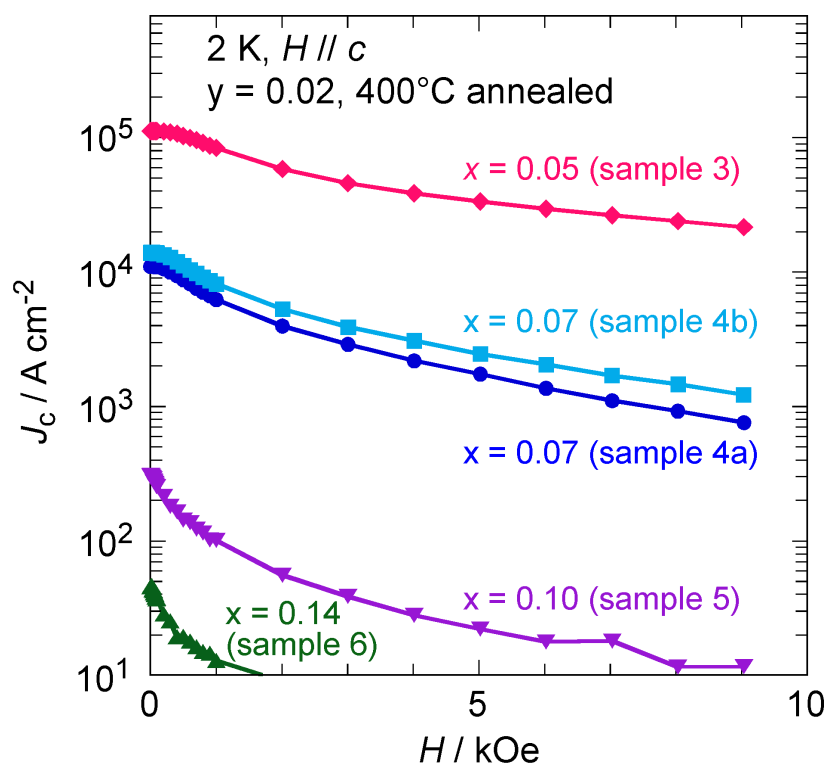


Fig. 6